Affine Term Structure Pricing with Bonds Supply As Factors

by

Fumio Hayashi

National Graduate Institute for Policy Studies, Japan, and National Bureau of Economic Research

March 2016

Abstract

This paper presents a theoretical model for analyzing the effect of the maturity structure of government debt on the yield curve. It is an ATSM (affine term structure model) in which the factors for the yield curve include, in addition to the short rate, the government bond supply for each maturity. The supply shock is not restricted to be perfectly correlated across maturities. The effect on the yield curve of a bond supply shock that is local to a maturity is largest at the maturity. This hump-shaped response of the yield curve obtains in spite of the absence of preferred-habitat investors.

Keywords: ATSM, yield curve, portfolio balance channel, supply of government bonds, impulse responses.

I thank Junko Koeda for posing the question studied in this paper and participants at a Kyoto University workshop. The research reported here was supported by grants-in-aid from the Ministry of Education, Culture, Sports, Science, and Technology of the Japanese government (grant number 25285097 and 26870124).

1 Introduction

How does the maturity structure of government debt affect the yield curve? The question has recently gained prominence due to the arrival of unconventional monetary policy, whose main aim is to lower the long-term interest rates by making the supply of long-term bonds scarce through reserve-financed open-market purchases. The theoretical justification often cited by central bankers is the *portfolio balance channel*.[1] This paper provides a formulation of it.

To be sure, such a channel cannot exist according to the irrelevance theorem of Wallace (1981). However, recent theoretical studies show that it can be reconnected if suitable transactions costs are considered,[2] and recent empirical studies on the effect of unconventional monetary policy find that the maturity structure matters for the yield curve.[3]

This paper proceeds under the assumption that relevant transactions costs exist so that the bond market can be studied in isolation. More specifically, it is closely related to the recent explicit models of the bond market by Vayanos and Villa (2009) and, especially, Greenwood and Vayanos (2014). The model in the former has two types of bond investors: arbitrageurs with the mean-variance preferences and preferred-habitat investors for each maturity. The net supply of bonds is zero for each maturity. An attractive feature of the model is that the equilibrium yields are affine functions of the factors that drive the short rate and the preferred-habitat investors' demand for bonds of various maturities, thus providing a link to the ATSM (affine term structure model), the reigning theory of the yield curve in finance.

Greenwood and Vayanos (2014, GV henceforce) simplify Vayanos and Vila (2009) by assuming that the preferred-habitat investors' demand is price-inelastic, or equivalently, by replacing the preferred habitats by an entity that sets the supply of bonds of various maturities inelastically. That entity can be interpreted as the government composed of the treasury and the central bank. Let b_n be the loading (the coefficient in the affine equation) on the supply factor for the yield of maturity n. GV show that (i) an increase in the supply factor raises all yields (i.e., $b_n > 0$ for all n) (ii) the profile

[1] To cite Bernanke (2010): "I see the evidence as most favorable to the view that such purchases work primarily through the so-called *portfolio balance channel* [italics by the author]... Specifically, the Fed's strategy [the operation twist] relies on the presumption that different financial assets are not perfect substitutes in investors' portfolios, so that changes in the net supply of an asset available to investors affect its yield and those of broadly similar assets."

[2] See Andres, Lopez-Salido, and Nelson (2004) and Chen, Curdia, and Ferrero (2012).

[3] For a list of recent empirical studies, see the survey in Woodford (2012) and also Bauer and Rudebusch (2014).

of this supply effect can be hump-shaped (i.e., b_n is increasing and then decreasing in n), (iii) for the risk premium, its profile is increasing across all maturities (i.e., the b_n for the risk premium is an increasing function of n), and (iv) it lies above the yield profile (i.e., the b_n for the risk premium is greater than the b_n for the yield for all n).

Our paper differs from GV in two respects.[4] First, the supply factor in GV is one-dimensional, while in our model there can be as many supply factors as there are maturities. Put differently, the maturity structure in GV is controlled by the global factor, while in our model the supply shock can be local, not restricted to be perfectly correlated across maturities. Despite the vastly expanded list of factors, the yields are still affine in the factors. Second, instead of characterizing the factor loadings, we employ the IR (impulse response) analysis to describe the dynamic version of the four results mentioned above (suitably modified to accommodate by local supply factors). We can thus examine the dynamic effect on the yield curve of what we call the "legacy" feature of bond supply that n-period bonds purchased by the government form part of the stock of $n-1$ period bonds next period barring an offsetting market operation.

The rest of the paper is organized as follows. Section 2 is a restatement in discrete time of GV's continuous-time model. Section 3 and the two appendixes show how multiple supply shocks can be incorporated into the model of GV. Section 4 conducts the IR analysis. Section 5 is a brief conclusion.

---

2 The Greenwood-Vayanos Model in Discrete Time

We first present the discrete-time version of the bond pricing model of Greenwood and Vayanos (2014) (hereafter, GV). Denote by $P_t^{(n)}$ the price of the zero-coupon bond with maturity n in period t. By convention, $P_t^{(0)} = 1$. The (continuously compounded) yield to maturity $y_t^{(n)}$ is therefore

$$y_t^{(n)} = -\frac{1}{n}\log P_t^{(n)}. \tag{2.1}$$

The nominal share of the n-period bond supplied is denoted by $s_t^{(n)}$. The longest maturity of bonds supplied is N. The shares add up to 1 (i.e., $\sum_{n=1}^{N} s_t^{(n)} = 1$) but some shares can be negative. The profile $(s_t^{(2)}, s_t^{(3)}, ..., s_t^{(N)})$ will be referred to as the *maturity structure* of bonds supplied.

Those bonds are traded by arbitrageurs. If $z_t^{(n)}$ is the nominal share of their n-period bond

[4]Like Vayanos and Vila (2009) and GV, our model ignores the zero lower bound for the interest rates. See Hamilton and Wu (2012) and Koeda (2015) for how the lower bound can be incorporated in the model of Vayanos and Vila (2009).

holdings, the (one plus) holding period return on their bond portfolio is

$$R_{t+1} \equiv \sum_{n=1}^{N} \frac{P_{t+1}^{(n-1)} - P_t^{(n)}}{P_t^{(n)}} z_t^{(n)}. \tag{2.2}$$

The arbitrageurs' decision problem is to maximize this risk-adjusted portfolio return subject to the adding-up constraint:[5]

$$\max_{\{z_t^{(n)}\}_{n=1}^N} \left[\mathrm{E}_t(R_{t+1}) - \frac{\gamma}{2} \operatorname{Var}_t(R_{t+1}) \right] \quad \text{subject to} \quad \sum_{t=1}^{N} z_t^{(n)} = 1. \tag{2.3}$$

Here, γ is a risk-aversion coefficient.

The bond market equilibrium is that $z_t^{(n)} = s_t^{(n)}$ for $n = 1, 2, ..., N$. With the arbitrageurs caring only about the portfolio return and with the maturity structure exogenously given by the government, there are no preferred-habitat investors in the model. Because of the adding-up constraint $\sum_{t=1}^{N} z_t^{(n)} = 1$, only $N - 1$ of these equilibrium conditions are independent. In GV and many others, the shortest yield $y_t^{(1)}$ is exogenous, being determined outside the model.

The equilibrium bond prices are assumed to be a time-invariant function of a vector, $\mathbf{f}_t$, of factors whose dynamics is given by a Gaussian VAR(1):

$$\mathbf{f}_{t+1} = \mathbf{c} + \mathbf{\Phi}\, \mathbf{f}_t + \boldsymbol{\varepsilon}_{t+1}, \quad \boldsymbol{\varepsilon}_t \sim \mathcal{N}(\mathbf{0}, \mathbf{\Omega}). \tag{2.4}$$

The state vector $\mathbf{f}_t$ in GV is two-dimensional. The first factor determines the shortest yield $y_t^{(1)}$. The second factor is a *single* variable that drives the maturity structure.[6] It is a global supply factor because bonds supplied at two different maturities are perfectly correlated. GV show that, as in the standard ATSM (affine term structure model), the time-invariant function is exponential affine, that is,

$$\log P_t^{(n)} = \bar{a}_n + \bar{\mathbf{b}}_n' \mathbf{f}_t, \;\; \text{so by (2.1),} \;\; y_t^{(n)} = a_n + \mathbf{b}_n' \mathbf{f}_t \;\; \text{where} \;\; a_n \equiv -\frac{\bar{a}_n}{n}, \; \mathbf{b}_n \equiv -\frac{\bar{\mathbf{b}}_n}{n}, \quad n = 1, 2, ..., N. \tag{2.5}$$

[5]We follow the discrete-time formulation by Hamilton and Wu (2012) of Vayanos and Vila (2009) to take R_{t+1} to be the portfolio return rather than the increase in wealth. In the latter case, $z_t^{(n)}$ is the level of nominal investment in bonds of maturity n. We are thus normalizing R_{t+1} and $z_t^{(n)}$ to the initial wealth. We do this because the model's calibration later in the paper is more straightforward.

[6]More precisely,

$$s_t^{(n)} = \zeta(n) + \theta(n) f_{2t}, \quad n = 1, 2, ..., N,$$

where $\zeta(n)$ and $\theta(n)$ are deterministic function of n and f_{2t} is the second factor.

3 Affine Bond Pricing with Bonds Supply as Factors

We modify the model of GV and allow the bond supply to have local actors that are specific to each maturity. This is accomplished by treating the maturity structure as additional factors. We show that the bond prices are exponential affine as in (2.5), even with this expanded state vector $\mathbf{f}_t$.

As in Vayanos and Vila (2009), GV, and many others, we proceed in two steps:

(a) Derive the arbitrageurs' FOCs (first-order conditions) that involve the affine coefficients $(\bar{a}_n, \bar{\mathbf{b}}_n)$ under the VAR dynamics (2.4) and the conjecture of the affine bond pricing (2.5).

(b) Impose on the FOC the bond market equilibrium conditions, $z_t^{(n)} = s_t^{(n)}$ for $n = 2, 3, ..., N$, to derive a set of equations for the affine coefficients.

Regarding (a), the FOCs for n-period bonds are (see Appendix 1 for a derivation)

$$\underbrace{\underbrace{\mathrm{E}_t\left[\frac{P_{t+1}^{(n-1)} - P_t^{(n)}}{P_t^{(n)}}\right]}_{\text{holding-period return}} - \underbrace{\frac{1 - P_t^{(1)}}{P_t^{(1)}}}_{\text{short rate}}}_{\text{risk premium on } n\text{-period bonds}} = \gamma \, \frac{1}{2} \, \frac{\partial \, \mathrm{Var}_t(R_{t+1})}{\partial z_t^{(n)}}, \quad n = 2, 3, ..., N, \tag{3.1}$$

which captures the trade-off between risk and return: the higher the risk-aversion coefficient γ, the more risk premium demanded by arbitrageurs. Using (2.4) and (2.5), we can rewrite the risk premium (the left-hand side of (3.1)) and $\frac{1}{2}\frac{\partial \, \mathrm{Var}_t(R_{t+1})}{\partial z_t^{(n)}}$ (the right-hand side of (3.1)) as

$$\mathrm{E}_t\left[\frac{P_{t+1}^{(n-1)} - P_t^{(n)}}{P_t^{(n)}}\right] - \frac{1 - P_t^{(1)}}{P_t^{(1)}} \approx \mathrm{E}_t\left(\log P_{t+1}^{(n-1)}\right) - \log P_t^{(n)} + \frac{1}{2}\bar{\mathbf{b}}_{n-1}' \boldsymbol{\Omega} \bar{\mathbf{b}}_{n-1} - y_t^{(1)} \tag{3.2}$$

$$= \bar{a}_{n-1} + \bar{\mathbf{b}}_{n-1}' \left(\mathbf{c} + \boldsymbol{\Phi} \mathbf{f}_t\right) - \bar{a}_n - \bar{\mathbf{b}}_n' \mathbf{f}_t + \frac{1}{2}\bar{\mathbf{b}}_{n-1}' \boldsymbol{\Omega} \bar{\mathbf{b}}_{n-1} + \bar{a}_1 + \bar{\mathbf{b}}_1' \mathbf{f}_t,$$

$$= \left(\bar{a}_{n-1} + \bar{\mathbf{b}}_{n-1}' \mathbf{c} - \bar{a}_n + \frac{1}{2}\bar{\mathbf{b}}_{n-1}' \boldsymbol{\Omega} \bar{\mathbf{b}}_{n-1} + \bar{a}_1\right) + \left(\mathbf{b}_{n-1}' \boldsymbol{\Phi} - \bar{\mathbf{b}}_n' + \bar{\mathbf{b}}_1'\right) \mathbf{f}_t, \tag{3.3}$$

$$\frac{1}{2}\,\frac{\partial \, \mathrm{Var}_t(R_{t+1})}{\partial z_t^{(n)}} \approx \bar{\mathbf{b}}_{n-1}' \boldsymbol{\Omega} \left(\bar{\mathbf{b}}_1 z_t^{(2)} + \cdots + \bar{\mathbf{b}}_{N-1} z_t^{(N)}\right). \tag{3.4}$$

These expressions, while exact in continuous time, are only approximations in discrete time.[7]

Turning to (b), upon the imposition of the market equilibrium conditions, the expression (3.4) of

[7] The derivation can be found in Hamilton and Wu (2012). For the sake of completeness, Appendix 1 has a derivation.

$\frac{1}{2}\frac{\partial \operatorname{Var}_t(R_{t+1})}{\partial z_t^{(n)}}$ can be written as (with F denoting the dimension of $\mathbf{f}_t$)

$$
\begin{aligned}
\frac{1}{2}\frac{\partial \operatorname{Var}_t(R_{t+1})}{\partial z_t^{(n)}} &\approx \underset{(1\times F)}{\bar{\mathbf{b}}'_{n-1}} \underset{(F\times F)}{\mathbf{\Omega}} \underbrace{\left(\bar{\mathbf{b}}_1 s_t^{(2)} + \cdots + \bar{\mathbf{b}}_{N-1} s_t^{(N)}\right)}_{(F\times 1)} \qquad \text{(by replacing } z_t^{(i)} \text{ by } s_t^{(i)},\ i = 2, ..., N) \\
&= \underset{(1\times F)}{\bar{\mathbf{b}}'_{n-1}} \underset{(F\times F)}{\mathbf{\Omega}} \underbrace{\begin{bmatrix} \bar{\mathbf{b}}_1 & \bar{\mathbf{b}}_2 & \cdots & \bar{\mathbf{b}}_{N-1} \end{bmatrix}}_{(F\times(N-1))} \underbrace{\begin{bmatrix} s_t^{(2)} \\ s_t^{(3)} \\ \vdots \\ s_t^{(N)} \end{bmatrix}}_{((N-1)\times 1)} \\
&= \underset{(1\times F)}{\bar{\mathbf{b}}'_{n-1}} \underset{(F\times F)}{\mathbf{\Omega}} \underbrace{\begin{bmatrix} \bar{\mathbf{b}}_1 & \bar{\mathbf{b}}_2 & \cdots & \bar{\mathbf{b}}_{N-1} \end{bmatrix}}_{(F\times(N-1))} \underset{((N-1)\times F)}{\mathbf{S}} \underset{(F\times 1)}{\mathbf{f}_t}.
\end{aligned} \tag{3.5}
$$

The key here is to use the selection matrix $\mathbf{S}$ to extract the maturity structure $(s_t^{(2)}, s_t^{(3)}, ..., s_t^{(N)})$ from $\mathbf{f}_t$.[8]

Substituting (3.3) and (3.5) into (3.1), we obtain an equation that is affine in $\mathbf{f}_t$. This has to hold for any $\mathbf{f}_t$. Setting both the constant term and the coefficients of $\mathbf{f}_t$ to zero, we obtain

$$
\underset{(1\times F)}{\bar{\mathbf{b}}'_n} = \underset{(1\times F)}{\bar{\mathbf{b}}'_{n-1}} \underset{(F\times F)}{\mathbf{\Phi}} - \gamma \underset{(1\times F)}{\bar{\mathbf{b}}'_{n-1}} \underset{(F\times F)}{\mathbf{\Omega}} \underbrace{\begin{bmatrix} \underset{(F\times 1)}{\bar{\mathbf{b}}_1} & \underset{(F\times 1)}{\bar{\mathbf{b}}_2} & \cdots & \underset{(F\times 1)}{\bar{\mathbf{b}}_{N-1}} \end{bmatrix}}_{(F\times(N-1))} \underset{((N-1)\times F)}{\mathbf{S}} + \underset{(1\times F)}{\bar{\mathbf{b}}'_1}, \quad n = 2, 3, ..., N, \tag{3.7}
$$

$$
\bar{a}_n = \bar{a}_{n-1} + \underset{(1\times F)}{\bar{\mathbf{b}}'_{n-1}} \underset{(F\times 1)}{\mathbf{c}} + \frac{1}{2} \underset{(1\times F)}{\bar{\mathbf{b}}'_{n-1}} \underset{(F\times F)}{\mathbf{\Omega}} \underset{(F\times 1)}{\bar{\mathbf{b}}_{n-1}} + \bar{a}_1, \quad n = 2, 3, ..., N. \tag{3.8}
$$

Given an initial condition about $\bar{\mathbf{b}}_1$, equation (3.7) determines the factor loading coefficients $\bar{\mathbf{b}}_n$, $n = 2, 3, ..., N$. Given an initial condition about $\bar{a}_1$ and given the factor loadings ($\bar{\mathbf{b}}'s$) thus determined, the recursion (3.8) generates $\bar{a}_n$, $n = 2, 3, ..., N$. Unlike in the standard textbook ATSM and in contrast to (3.8), equation (3.7) is not a recursion thanks to the quadratic term (the second term on the right-hand side of the equation); it is a QVE (quadratic vector equation). Appendix 2 shows how we solved this QVE.

Before closing this section, we note for later reference that there is a link between yields and risk premia. Define the risk premium $\mathrm{rp}_t^{(n)}$ by the right-hand side of (3.2). The usual forward iteration

[8] If $(s_t^{(2)}, s_t^{(3)}, ..., s_t^{(N)})$ are placed last in $\mathbf{f}_t$, the $\mathbf{S}$ matrix can be written as

$$
\underset{((N-1)\times F)}{\mathbf{S}} = \begin{bmatrix} \underset{((N-1)\times(F-(N-1)))}{\mathbf{0}} & \mathbf{I}_{N-1} \end{bmatrix}. \tag{3.6}
$$

argument then yields:[9]

$$y_t^{(k)} = \frac{1}{k}\sum_{i=0}^{k-1} \mathrm{E}_t\Big(y_{t+i}^{(1)} + \mathrm{rp}_{t+i}^{(k-i)}\Big) + \frac{1}{k}A_k, \quad k = 1, 2, ..., N, \tag{3.9}$$

where $A_k \equiv -\frac{1}{2}\sum_{i=0}^{k-1} \bar{\mathbf{b}}'_{k-i-1}\boldsymbol{\Omega}\bar{\mathbf{b}}_{k-i-1}$.

---

4 Impulse Responses

Our model's parameters are: γ (the arbitrageurs' risk-aversion coefficient), N (the maximum maturity), and $(\mathbf{c}, \boldsymbol{\Phi}, \boldsymbol{\Omega})$ (the VAR parameters describing the factor dynamics). The previous section and Appendix 2 were about how to map the model parameters to the affine yield curve coefficients $(a_n, \mathbf{b}_n, n = 1, 2, ..., N)$ through the QVE (3.7) and the recursion (3.8) in $\{a_n\}$. In this section, we calculate the IR (impulse response) of the yield curve to shocks originating in the maturity structure.

Specifying the Factor Dynamics

The example we consider has only one factor besides the maturity structure. Without loss of generality, we can take that non-supply factor to be the short rate $y_t^{(1)}$. Thus F (the number of factors) equals N, and the factors are given by

$$\underset{(N\times 1)}{\mathbf{f}_t} = \Big(y_t^{(1)}, s_t^{(2)}, s_t^{(3)}, ..., s_t^{(N)}\Big)'. \tag{4.1}$$

With this choice of the factor vector, the initial condition to be fed to the recursion (3.8) and the QVE (quadratic vector equation) (3.7) is given by

$$\bar{a}_1 = 0, \;\; \bar{\mathbf{b}}'_1 = (1, 0, ..., 0). \tag{4.2}$$

---

[9]By the definition of $\mathrm{rp}_t^{(k)}$, we have

$$\mathrm{E}_t\Big(\log P_{t+1}^{(k-1)}\Big) - \log P_t^{(k)} - y_t^{(1)} = \mathrm{rp}_t^{(k)} - \frac{1}{2}\bar{\mathbf{b}}'_{n-1}\boldsymbol{\Omega}\bar{\mathbf{b}}_{k-1}.$$

The usual forward iteration trick with the terminal condition $\log P_{t+k}^{(0)} = 0$ yields

$$-\log P_t^{(k)} = \sum_{i=0}^{k-1} \mathrm{E}_t\Big(y_{t+i}^{(1)} + \mathrm{rp}_{t+i}^{(k-i)} - \frac{1}{2}\bar{\mathbf{b}}'_{k-i-1}\boldsymbol{\Omega}\bar{\mathbf{b}}_{k-i-1}\Big).$$

(3.9) obtains because $y_t^{(k)} = -\frac{1}{k}\log P_t^{(k)}$.

The VAR dynamics are specified as

$$\text{(short rate)} \qquad y_t^{(1)} = c_1 + \rho y_{t-1}^{(1)} + \varepsilon_{1t}, \quad \varepsilon_{1t} \sim \mathcal{N}(0, \sigma_1^2), \tag{4.3}$$

$$\text{(maturity structue)} \qquad s_t^{(n)} = \begin{cases} c_n + \theta s_{t-1}^{(n+1)} + \varepsilon_{nt}, \quad \varepsilon_{nt} \sim \mathcal{N}(0, \sigma_n^2) & \text{if } n = 2, 3, ..., N-1, \\ c_N + \varepsilon_{Nt}, \quad \varepsilon_{Nt} \sim \mathcal{N}(0, \sigma_N^2) & \text{if } n = N. \end{cases} \tag{4.4}$$

Here, the supply shocks (ε_{1t},...,ε_{Nt}) are uncorrelated.[10] Four points about the dynamics.

- Since the bond supply shocks ($\varepsilon_{2t}, ..., \varepsilon_{Nt}$) are uncorrelated across maturities, each of them represent a purely local supply shock in the maturity spectrum.
- The short rate is exogenous because there is no feedback to the short rate from the maturity structure and the short rate shock ε_{1t} is uncorrelated with the bond supply shocks. Therefore, the response of the yield curve to a bond supply shock would represent what is referred to as the portfolio balance effect.
- The maturity structure dynamics (4.4) captures the "legacy" property of bonds that an n-period bond becomes an $n-1$-period bond next period. The strength of legacy is represented by θ.

Calibration

To avoid heavy demand on CPU time, we choose the unit interval to be a quarter, not a month. So $y_t^{(1)}$ is the 3-month interest rate. We set N to be 80 quarters (20 years). For calibration purposes we use the U.S. Treasury zero-coupon yield curve calculated by Gurkaynak, Sack, and Wright (2007).[11]

---

[10] The implied restrictions on the factor dynamics parameters ($\mathbf{c}, \mathbf{\Phi}, \mathbf{\Omega}$) are as follows.

$$\underset{(N\times 1)}{\mathbf{c}} = (c_1, c_2, ..., c_{N-1}, c_N)', \quad \underset{(N\times N)}{\mathbf{\Phi}} = \begin{bmatrix} \rho & \underset{(1\times(N-1))}{\mathbf{0}'} \\ \underset{((N-1)\times 1)}{\mathbf{0}} & \underset{((N-1)\times(N-1))}{\tilde{\mathbf{\Phi}}} \end{bmatrix}, \quad \underset{(N\times N)}{\mathbf{\Omega}} = \begin{bmatrix} \sigma_1^2 & \underset{(1\times(N-1))}{\mathbf{0}'} \\ \underset{((N-1)\times 1)}{\mathbf{0}} & \underset{((N-1)\times(N-1))}{\tilde{\mathbf{\Omega}}} \end{bmatrix},$$

where $\tilde{\mathbf{\Omega}} = \text{diag}\{\sigma_2^2, ..., \sigma_N^2\}$ and $\tilde{\mathbf{\Phi}}$ is given by

$$\underset{((N-1)\times(N-1))}{\tilde{\mathbf{\Phi}}} = \begin{bmatrix} 0 & \theta & 0 & 0 & \cdots & 0 \\ 0 & 0 & \theta & 0 & \cdots & 0 \\ \vdots & \vdots & \ddots & \ddots & \ddots & 0 \\ 0 & 0 & \cdots & 0 & \theta & 0 \\ 0 & 0 & \cdots & \cdots & 0 & \theta \\ 0 & 0 & \cdots & \cdots & \cdots & 0 \end{bmatrix}.$$

[11] The parameterized function used to fit the yields of various observed maturities is given as equation (22) in Gurkaynak *et. al.* (2007). The daily parameter values can be downloaded from the Federal Reserve Board

The values for (c_1, ρ, σ_1) are obtained from an AR1 estimation on the short rate. Our results to be reported below are sensitive to the calibrated values for those parameters, particularly for σ_1, which in turn depend on the choice of the sample period. We report results based on the period under Alan Greenspan's chairmanship (1987:Q3 - 2005:Q4). The estimated AR1 model is (with standard errors in parentheses)

$$y_t^{(1)} = \underset{(0.00037)}{0.0003829} + \underset{(0.029)}{0.9592}\, y_{t-1}^{(1)}, \quad \text{S.E.R} = 0.001291, \quad t = \text{1987:Q4-2005:Q4}. \tag{4.5}$$

($y_t^{(1)}$ is expressed as a rate per quarter.) This estimated AR1 determiens ρ and σ_1: $\rho = 0.9592$, and $\sigma_1 = 0.001291$. The value of c_1 is set so that the AR1 process's steady-state value, $c_1/(1-\rho)$, equals the sample mean over 1987:Q3-2005:Q4 of $y_1^{(1)}$.[12]

We pick $(c_2, ..., c_N)$ so that the steady-state value of $s_t^{(n)}$ is $1/N$ for $n = 2, ..., N$.[13] We set $\sigma_n = \lambda/N$ with $\lambda = 0.01$ for $n = 2, 3, ..., N$. The affine coefficients turned out to be fairly insensitive to λ; for both the yield curve and the risk premium, the results about the level and the IR to a supply shock of a fixed size (we will consider a 1 percentage point shock to $s_t^{(n)}$) are very similar for a wide range of λ including $[0.001, 0.1]$.

This leaves two parameters, γ (the risk aversion parameter) and θ (which controls the maturity structure dynamics). As it turns out, the latter has no effect on the steady-state yield curve (the yield curve given by the affine equation (2.5) when $\mathbf{f}_t$ equals to its steady-state value).[14] We can therefore

---

website. From this we can calculate $y_t^{(n)}$ for any maturity n. We take the yield for the quarter to be for the last business day of the quarter. For the short rate we use the value implied by the parameterized yield curve at $n = 1$ (3 months). This short rate series is very similar to the constant-maturity 3-month rate available from Federal Reserve Board's Table H-15.

[12]Let $\bar{y}$, $\bar{\bar{y}}$, and $\tilde{y}$ be the sample mean of $y_t^{(1)}$ over 1987:Q3-2005:Q4, 1987:Q4-2005:Q4, and 1987:Q3-2005:Q3, respectively. Let $\hat{c}_1$ and $\hat{\rho}$ be the AR1 estimates shown in (4.5) of c_1 and ρ (so $\hat{c}_1 = 0.0003829$ and $\hat{r} = 0.9592$). Then $\bar{\bar{y}} = \hat{c}_1 + \hat{\rho}\hat{y}$, or $\hat{c}_1/(1-\hat{\rho}) = \hat{y} - (\hat{y} - \bar{\bar{y}})/(1-\hat{\rho})$. In our sample, the three sample means are different enough to make $\hat{c}_1/(1-\hat{\rho})$ deviate substantially from the sample mean $\bar{y}$. ($\hat{c}_1/(1-\hat{\rho}) = 3.75\%$ in APR while $\bar{y} = 4.64\%$ in APR.) So, instead of setting $c_1 = \hat{c}_1$, we choose c_1 so that $c_1/(1-\hat{\rho}) = \bar{y}$.

[13] Let $\underset{((N-1)\times 1)}{\mathbf{s}_t} \equiv (s_t^{(2)}, ..., s_t^{(N)})'$ be the maturity structure, $\tilde{\mathbf{c}} \equiv (c_2, ..., c_{N-1}, c_N)'$, and let $\tilde{\mathbf{\Phi}}$ be as in footnote 10. Then the steady-state value of $\mathbf{s}_t$, call it $\mathbf{s}$, satisfies: $(\mathbf{I} - \tilde{\mathbf{\Phi}})\mathbf{s} = \tilde{\mathbf{c}}$.

[14]As noted in the text and in footnote 13, we chose $(c_2, ..., c_N)$ so that the maturity structure in the steady state is flat. Thus the factor vector in the steady state is

$$\text{factor vector in the steady state} = \Big(\frac{c_1}{1-\rho}, \underbrace{\frac{1}{N}, ..., \frac{1}{N}}_{N-1 \text{ terms}}\Big).$$

If the staedy-state maturity structure is flat, as here, then θ does not affect the steady-state yield curve given calibrate γ to the steady-state yield curve without specifying the value of θ. We set $\gamma = 52/4$ (or $\gamma = 52$ if the quarterly portfolio return R_{t+1} in (2.3) is expressed at an annual rate) because, as shown in **Figure 1**, the steady-state yield curve and the corresponding sample mean for the sample period (1987:Q3 - 2005:Q4) are reasonably close to each other under this value of γ.[15]

Impulse Responses

The N-dimensional factor dynamics consisting of (4.3) and (4.4) has the IR (impulse response) function of $\mathbf{f}_t$ to the bond supply shocks $(\varepsilon_2, ..., \varepsilon_N)$ given by

$$\underbrace{\frac{\partial \mathbf{f}'_{t+j}}{\partial \varepsilon_{nt}}}_{(1\times N)} = \begin{cases} (0, 0, ..., 0, \underset{(n-j)}{\theta^j}, 0, ..., 0) & \text{for} \quad j = 0, 1, ..., n-2, \ \text{(with } \theta^j = 1 \text{ for } \theta = 0 \text{ and } j = 0\text{)}, \\ \underset{(1\times N)}{\mathbf{0}'} & \text{for} \quad j = n-1, n, ... \end{cases} \tag{4.6}$$

$$\text{for } n = 2, 3, ..., N.$$

That is, a unit supply shock originating at maturity n becomes a supply shock of size θ^j at maturity $n - j$ in j periods, and gets absorbed at maturity 1 in $n - 1$ periods (recall that the short rate is exogenous to supply shocks).

The factor IR readily translates to the yield-curve IR via the affine equation (2.5). Thanks to the special feature of the factor IR, there is a tight connection between the factor loadings ($\mathbf{b}_n$'s in (2.5)) and the yield IR profile. The latter is a profile of N elements given by:

$$\underbrace{\frac{\partial \left(y^{(1)}_{t+j}, y^{(2)}_{t+j}, y^{(3)}_{t+j}, ..., y^{(N)}_{t+j}\right)}{\partial \varepsilon_{nt}}}_{(1\times N)} = \begin{cases} \underbrace{(0, b_{2,n-j}, b_{3,n-j} ..., b_{N,n-j})}_{(1\times N)} \theta^j & \text{for} \quad j = 0, 1, ..., n-2, \\ \underset{(1\times N)}{\mathbf{0}'} & \text{for} \quad j = n-1, n, ... \end{cases} \tag{4.7}$$

$$\text{for } n = 2, 3, ..., N,$$

where $b_{n,k}$ is the k-th element of $\underset{(N\times 1)}{\mathbf{b}_n}$. To understand this formula, imagine an $N \times N$ matrix whose columns are $[\mathbf{0}\ \mathbf{b}_2\ ...\ \mathbf{b}_N]$. The impact response profile (the profile for $j = 0$) is the n-th row of this matrix. The fifth row up from this row, if it is scaled by the legacy parameter θ^5, is the profile for $j = 5$, for example. The factor loadings for the short rate, $\mathbf{b}_1$, do not enter the profile because the short rate is exogenous. The legacy parameter θ, while irrelevant for the steady-state analysis,

by the affine equation (2.5), despite the fact that θ affects the affine coefficients $(a_n, \mathbf{b}_n)$ $(n = 2, 3, ..., N)$.

[15] This value of $\gamma = 52$ is close to the value for the same parameter calibrated by GV (Greenwood and Vayanos (2014)) of 57.

affects the IR profile in two ways: it scales the factor loadings (as just mentioned) and it is a determinant of the factor loadings themselves. Below we consider two values for θ: 0 and 1.

Assume first $\theta = 1$. The set of across-maturity profiles shown in the **left panel of Figure 2** are the yield IR profiles for $j = 0$ (the impact response), $j = 20$ (5 years out), $j = 40$ (10 years), and $j = 60$ (15 years). The shock considered here originates at the longest maturity with $n = N$ (= 80), with a shock size of 1 percentage point. With $\theta = 1$, (4.7) shows that the yield IR profile depends on n and j only thorough $n - j$. Therefore, for example, the IR profile after 15 years to a shock originating at $n = 80$ quarters (20 years) (the dashed profile in the panel) is also the impact response profile (the IR profile for $j = 0$) to a shock originating at $n = 20$ quarters (5 years).

As the panel shows, the IR profiles are hump-shaped, peaking near the maturity where the local supply shock originates. To explain why, it is useful to temporarily turn our attention to the risk premium.[16] Since, as seen from (3.3), the risk premium, too, is an affine function of the factor vector, the IR formula (4.7) can be used to calculate the IR of the risk premium if the factor loading coefficients $b_{n,k}$ are interpreted as the coefficients of $\mathbf{f}_t$ in (3.3). The **right panel of Figure 2** shows the risk-premium IR profiles for different horizons thus calculated. Two points to note.

- Unlike the yield IR profiles, which are hump-shaped, the risk-premium IR profiles are upward-sloping. The intuition is the same as given in GV (Greenwood and Vayanos (2014)) for factor loadings: since long-term bonds are more sensitive to duration risk than short-term bonds, the risk premium demanded by arbitrageurs must increase with the maturity. This explains why a local shock, no matter where in the maturity spectrum it originates, raises the risk premium for long-term bonds. This is illustrated for the impact response profile with the originating maturity n of 20 (5 years) by the dashed profile in the right panel.
- For all j, the risk-premium IR profile lies above the yield IR profile.

This last point follows from the relationship shown in (3.9) that the current yield is the average of the risk premium over the bond's life. Replacing t by $t + j$ in the formula and differentiating both sides with respect to the bond supply shock at the originating maturity n, ε_{nt}, and noting that the shock does not affect the future short rates, we obtain a link between the yield and the risk-premium IRs:

$$\frac{\partial y_{t+j}^{(k)}}{\partial \varepsilon_{nt}} = \frac{1}{k}\left[\frac{\partial\, \mathrm{rp}_{t+j}^{(k)}}{\partial \varepsilon_{nt}} + \frac{\partial\, \mathrm{rp}_{t+j+1}^{(k-1)}}{\partial \varepsilon_{nt}} + \cdots + \frac{\partial\, \mathrm{rp}_{t+j+k-2}^{(2)}}{\partial \varepsilon_{nt}} + \frac{\partial\, \mathrm{rp}_{t+j+k-1}^{(1)}}{\partial \varepsilon_{nt}}\right], \quad k = 1, 2, ..., N. \tag{4.8}$$

[16] A similar argument can be found in GV (Greenwood and Vayanos (2014), see the introduction) for factor loadings.

The yield IR, $\frac{\partial y_{t+j}^{(k)}}{\partial \varepsilon_{nt}}$, is less than the risk-premium IR, $\frac{\partial \,\mathrm{rp}_{t+j}^{(k)}}{\partial \varepsilon_{nt}}$, because it is the average of a declining sequence whose first term is the risk-premium IR.[17]

A similar reasoning explains the hump-shaped yield IR profiles. If the risk-premium IR profile were flat so that $\frac{\partial \,\mathrm{rp}_{t+j}^{(k)}}{\partial \varepsilon_{nt}}$ did not depend on the maturity k, then the average in (4.8) would be declining in k and the yield IR profile would be downward-sloping. But the risk-premium IR profile is upward sloping, which changes the sign of the slope for short maturities.

Finally, turn to the case $\theta = 0$. Since supply shocks are now temporary, only the impact response is non-zero for both the yield and the risk premium. The impact response profile is given by (4.7) for $j = 0$, which shows that it is invariant to θ ($\theta^j = 1$ for $j = 0$ regardless of θ). For example, in the right panel of Figure 2, the impact response profile for the risk premium to a supply shock originating at 20 quarters (5 years) is the dotted profile in the panel. Since the effect on the risk premium is temporary, as one can surmise from the formula (4.8), a local supply shock originating at any maturity has very little effect on the yield curve.

5 Conclusion

We have developed a model that provides a mapping from an arbitrary change in the maturity structure to the yield curve. The model can be viewed as a modern incarnation of Tobin's (1969) formulation of portfolio balance channel. Unlike in Tobin's, the mapping is explicitly tied to the dynamics of the supply factors, so that the strength of the portfolio channel can be made a function of the persistence of the supply shock.

[17] The sequence is declining because, as shown in the right panel of Figure 2, $\frac{\partial \,\mathrm{rp}_{t+j}^{(k)}}{\partial \varepsilon_{nt}}$ declines as k falls given j and as j increases given k.

Figure 1: Average Yield Curve

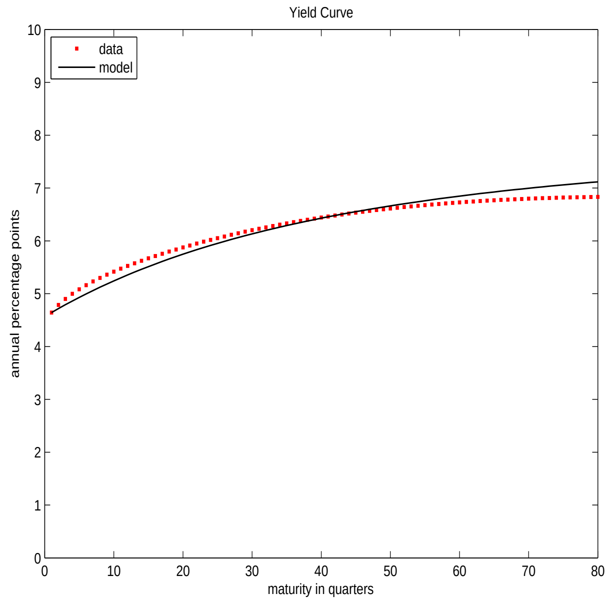

Note: The solid line is the steady-state yield curve implied by the model. The filled-in squares are the sample means from data.

Figure 2: Impulse Responses, $\theta = 1$

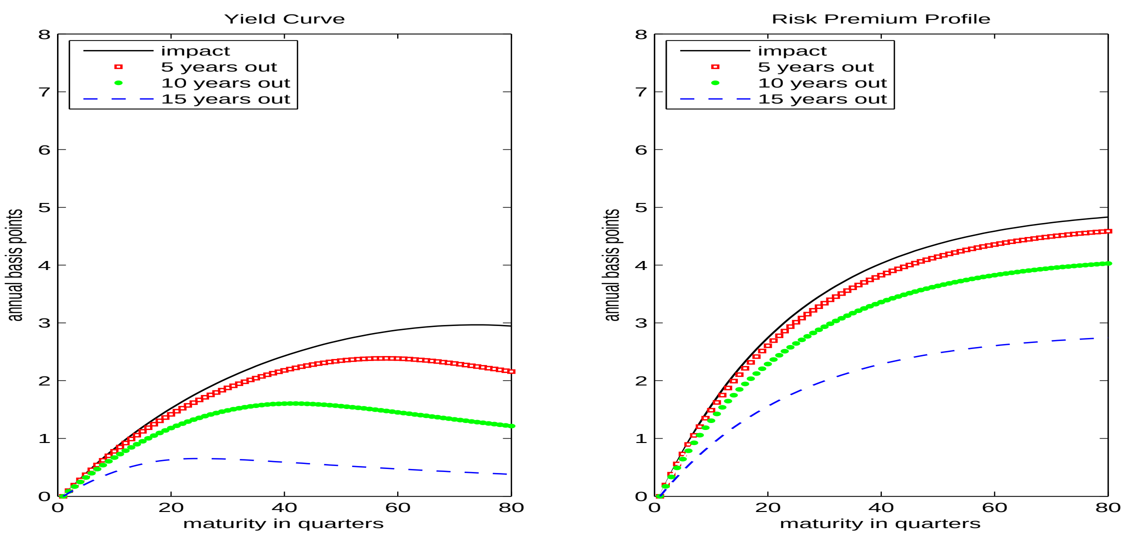

Note: The profiles across maturities of the impulse responses of the yield and the risk premium. The shock is a 1 percentage point increase in the share of 20-year bonds in the maturity structure.

Appendix 1 Derivation of (3.1)**,** (3.2)**, and** (3.4)

The arbitrageurs's decision problem is described by (2.3) with (2.2) of the text. If ϕ_t is the Lagrange multiplier for the constraint $\sum_{n=1}^{N} z_t^{(n)} = 1$, the FOCs (first-order conditions) are

$$\mathrm{E}_t\left[\frac{P_{t+1}^{(n-1)} - P_t^{(n)}}{P_t^{(n)}}\right] - \gamma\,\frac{1}{2}\,\frac{\partial\,\mathrm{Var}_t(R_{t+1})}{\partial z_t^{(n)}} \;=\; \phi_t, \quad n = 1, 2, ..., N, \tag{A1.1}$$

$$\sum_{n=1}^{N} z_t^{(n)} = 1. \tag{A1.2}$$

Since $P_{t+1}^{(0)} = 1$, the holding period return on the 1-period bond is $(1 - P_t^{(1)})/P_t^{(1)}$, which is known in date t. Hence $\frac{\partial\,\mathrm{Var}_t(R_{t+1})}{\partial z_t^{(n)}} = 0$ for $n = 1$ and the FOC for $n = 1$ is: $(1 - P_t^{(1)})/P_t^{(1)} = \phi_t$. Substituting this into the rest of the FOCs in (A1.1), we obtain (3.1) of the text, which is reproduced here:

$$\underbrace{\underbrace{\mathrm{E}_t\left[\frac{P_{t+1}^{(n-1)} - P_t^{(n)}}{P_t^{(n)}}\right]}_{\text{holding-period return}} \;-\; \underbrace{\frac{1 - P_t^{(1)}}{P_t^{(1)}}}_{\text{short rate}}}_{\text{risk premium on } n\text{-period bonds}} = \gamma\,\frac{1}{2}\,\frac{\partial\,\mathrm{Var}_t(R_{t+1})}{\partial z_t^{(n)}}, \quad n = 2, 3, ..., N, \tag{3.1}$$

In the rest of this appendix, we derive (3.2) and (3.4) under the VAR dynamics (2.4) and affine pricing (2.5). This can be done easily if we show the following.

- Show: $(1 - P_t^{(1)})/P_t^{(1)} \approx y_t^{(1)}$. This immediately follows from the approximation $1/x \approx 1 - \log(x)$ for $x \approx 1$ and the relation $y_t^{(1)} \equiv -\log P_t^{(1)}$.

- Let $p_t^{(n)} \equiv \log P_t^{(n)}$. Show: the distribution conditional on date t of $p_{t+1}^{(n-1)} - p_t^{(n)}$ is normal with mean $\bar{a}_{n-1} + \bar{\mathbf{b}}'_{n-1}(\mathbf{c} + \mathbf{\Phi}\mathbf{f}_t) - \bar{a}_n - \bar{\mathbf{b}}'_n\mathbf{f}_t$ and variance $\bar{\mathbf{b}}'_{n-1}\mathbf{\Omega}\bar{\mathbf{b}}_{n-1}$. This follows immediately from

$$p_{t+1}^{(n-1)} - p_t^{(n)} = \bar{a}_{n-1} + \bar{\mathbf{b}}'_{n-1}(\mathbf{c} + \mathbf{\Phi}\mathbf{f}_t) - \bar{a}_n - \bar{\mathbf{b}}'_n\mathbf{f}_t + \bar{\mathbf{b}}'_{n-1}\varepsilon_{t+1}, \tag{A1.3}$$

  which can be obtained by combining (2.4) and (2.5).

- Show:

$$\mathrm{E}_t\left[\frac{P_{t+1}^{(n-1)} - P_t^{(n)}}{P_t^{(n)}}\right] = \mathrm{E}_t\left[\exp(p_{t+1}^{(n-1)} - p_t^{(n)})\right] - 1 \approx \mathrm{E}_t\left(p_{t+1}^{(n-1)} - p_t^{(n)}\right) + \frac{1}{2}\,\mathrm{Var}_t\left(p_{t+1}^{(n-1)} - p_t^{(n)}\right). \tag{A1.4}$$

  This can be obtained easily from two well-known formulas. One is that, for a normally distributed random variable X, $\mathrm{E}[\exp(X)] = \exp[\mathrm{E}(X) + \frac{1}{2}\,\mathrm{Var}(X)]$, and the other is $\exp(x) \approx 1 + x$ for $x \approx 0$. In the former, we can set $X = p_{t+1}^{(n-1)} - p_t^{(n)}$ because, as shown above, $p_{t+1}^{(n-1)} - p_t^{(n)}$ is normally distributed conditional on date t information. In the latter formula, set $x = \mathrm{E}_t\left(p_{t+1}^{(n-1)} - p_t^{(n)}\right) + \frac{1}{2}\,\mathrm{Var}_t\left(p_{t+1}^{(n-1)} - p_t^{(n)}\right)$.

- Show:

$$\mathrm{Var}_t\,(R_{t+1}) \approx \mathbf{d}_t'\boldsymbol{\Omega}\mathbf{d}_t \quad \text{where} \quad \mathbf{d}_t \equiv \sum_{i=2}^{N} \bar{\mathbf{b}}_{i-1} z_t^{(i)}. \quad \text{So} \quad \frac{1}{2}\frac{\partial\,\mathrm{Var}_t(R_{t+1})}{\partial z_t^{(n)}} = \bar{\mathbf{b}}_{n-1}'\boldsymbol{\Omega}\mathbf{d}_t. \tag{A1.5}$$

To derive this, we again use the approximation $\exp(x) \approx 1 + x$ to derive

$$\frac{P_{t+1}^{(n-1)} - P_t^{(n)}}{P_t^{(n)}} = \exp\left(p_{t+1}^{(n-1)} - p_t^{(n)}\right) - 1 \approx p_{t+1}^{(n-1)} - p_t^{(n)}. \tag{A1.6}$$

Multiply both sides by $z_t^{(n)}$ and sum over $n = 1, 2, ..., N$ to obtain

$$\begin{aligned}
R_{t+1} \equiv \sum_{n=1}^{N} \frac{P_{t+1}^{(n-1)} - P_t^{(n)}}{P_t^{(n)}} z_t^{(n)} &\approx \sum_{n=1}^{N} \left(p_{t+1}^{(n-1)} - p_t^{(n)}\right) z_t^{(n)} \\
&= \underbrace{\sum_{n=1}^{N} \left[\bar{a}_{n-1} + \bar{\mathbf{b}}_{n-1}'\left(\mathbf{c} + \boldsymbol{\Phi}\mathbf{f}_t\right) - \bar{a}_n - \bar{\mathbf{b}}_n'\mathbf{f}_t\right] z_t^{(n)}}_{\equiv A_t} + \left(\sum_{n=1}^{N} \bar{\mathbf{b}}_{n-1}' z_t^{(n)}\right)\boldsymbol{\varepsilon}_{t+1} \\
&\qquad \text{(by (A1.3))} \\
&= A_t + \left(\sum_{n=1}^{N} \bar{\mathbf{b}}_{n-1}' z_t^{(n)}\right)\boldsymbol{\varepsilon}_{t+1} \qquad \text{(by the definition of } A_t \text{ right above)} \\
&= A_t + \left(\sum_{n=2}^{N} \bar{\mathbf{b}}_{n-1}' z_t^{(n)}\right)\boldsymbol{\varepsilon}_{t+1} \qquad \text{(since } \bar{\mathbf{b}}_0 = \mathbf{0}) \\
&= A_t + \mathbf{d}_t'\boldsymbol{\varepsilon}_{t+1} \qquad \text{(by the definition of } \mathbf{d}_t \text{ in (A1.5)).}
\end{aligned} \tag{A1.7}$$

Since A_t defined here is known in date t, the source of the date t conditional variance of R_{t+1} is the last term, $\mathbf{d}_t'\boldsymbol{\varepsilon}_{t+1}$.

Appendix 2 Solving the Quadratic Vector Equation (3.7)

To emphasize that we are dealing with a QVE (quadratic vector equation) in (3.7), define the NF-dimensional stacked vector $\bar{\mathbf{b}}$ as (recall: F is the number of factors)

$$\underset{(NF\times 1)}{\bar{\mathbf{b}}} \equiv \begin{bmatrix} \underset{(F\times 1)}{\bar{\mathbf{b}}_1} \\ \underset{(F\times 1)}{\bar{\mathbf{b}}_2} \\ \vdots \\ \underset{(F\times 1)}{\bar{\mathbf{b}}_N} \end{bmatrix}. \tag{A2.1}$$

Then it is straightforward to show that (3.7) and the initial condition $\bar{\mathbf{b}}_1 = \boldsymbol{\delta}$ together can be written as

$$\underset{(NF\times NF)}{\mathbf{M}}\;\underset{(NF\times 1)}{\bar{\mathbf{b}}} = \underset{(NF\times 1)}{\mathbf{d}} - \gamma \underset{(NF\times 1)}{\mathbf{g}(\bar{\mathbf{b}})}, \tag{A2.2}$$

where

$$\underset{(NF\times NF)}{\mathbf{M}} \equiv \begin{bmatrix} \mathbf{I}_F & \mathbf{0} & \mathbf{0} & \dots & \mathbf{0} \\ -\underset{(F\times F)}{\boldsymbol{\Phi}'} & \mathbf{I}_F & \mathbf{0} & \dots & \mathbf{0} \\ \mathbf{0} & -\underset{(F\times F)}{\boldsymbol{\Phi}'} & \mathbf{I}_F & \dots & \mathbf{0} \\ \vdots & & \ddots & \ddots & \mathbf{0} \\ \mathbf{0} & \dots & \mathbf{0} & -\underset{(F\times F)}{\boldsymbol{\Phi}'} & \mathbf{I}_F \end{bmatrix}, \tag{A2.3}$$

$$\underset{(NF\times 1)}{\mathbf{d}} \equiv \underset{(N\times 1)}{\mathbf{1}} \otimes \underset{(F\times 1)}{\boldsymbol{\delta}} \quad \text{(recall: } \boldsymbol{\delta} \text{ is the initial condition for } \bar{\mathbf{b}}_1\text{)}, \tag{A2.4}$$

$$\underset{(NF\times 1)}{\mathbf{g}(\bar{\mathbf{b}})} \equiv \begin{bmatrix} \underset{(F\times 1)}{\mathbf{0}} \\ \underbrace{\underset{(F\times(N-1))}{\mathbf{S}'}\;\underset{((N-1)\times F)}{\bar{\mathbf{B}}'}\;\underset{(F\times F)}{\boldsymbol{\Omega}}\;\underset{(F\times 1)}{\bar{\mathbf{b}}_1}}_{(F\times 1)} \\ \vdots \\ \underbrace{\underset{(F\times(N-1))}{\mathbf{S}'}\;\underset{((N-1)\times F)}{\bar{\mathbf{B}}'}\;\underset{(F\times F)}{\boldsymbol{\Omega}}\;\underset{(F\times 1)}{\bar{\mathbf{b}}_{N-1}}}_{(F\times 1)} \end{bmatrix} = \underset{(NF\times(N-1)^2)}{\mathbf{P}}\;\underbrace{\mathrm{vec}\left(\underbrace{\bar{\mathbf{B}}'\,\boldsymbol{\Omega}\,\bar{\mathbf{B}}}_{((N-1)\times(N-1))}\right)}_{((N-1)^2\times 1)},\quad \mathbf{P} \equiv \underbrace{\begin{bmatrix} \underset{(F\times(N-1)^2)}{\mathbf{0}} \\ \underbrace{\mathbf{I}_{N-1}\otimes \mathbf{S}'}_{((N-1)F\times(N-1)^2)} \end{bmatrix}}_{(NF\times(N-1)^2)}, \tag{A2.5}$$

$$\underset{(F\times(N-1))}{\bar{\mathbf{B}}} \equiv \begin{bmatrix} \underset{(F\times 1)}{\bar{\mathbf{b}}_1} & \underset{(F\times 1)}{\bar{\mathbf{b}}_2} & \cdots & \underset{(F\times 1)}{\bar{\mathbf{b}}_{N-1}} \end{bmatrix}. \tag{A2.6}$$

If $\gamma = 0$, the equation (3.7) or (A2.2) has a unique solution

$$\bar{\mathbf{b}}^* \equiv \mathbf{M}^{-1}\mathbf{d}. \tag{A2.7}$$

Although the square matrix $\mathbf{M}$, which is of size NF, can be large, computing $\bar{\mathbf{b}}^*$ is fast because there is a well-known analytical expression for the inverse of the large matrix $\mathbf{M}$.[18] If $\gamma > 0$, because of the quadratic term $\mathbf{g}(\bar{\mathbf{b}})$, there can be multiple solutions if a solution exists. Following GV (Greenwood and Vayanos (2014)), we seek the solution that converges to the unique solution $\bar{\mathbf{b}}^*$ as $\gamma \to 0$. To study such a solution for given $\gamma > 0$, write the equation as

$$\mathbf{f}(\bar{\mathbf{b}}, \gamma) = \underset{(NF\times 1)}{\mathbf{0}}, \quad \mathbf{f}(\bar{\mathbf{b}}, \gamma) \equiv \mathbf{M}\bar{\mathbf{b}} \; - \; \mathbf{d} \; + \; \gamma\, \mathbf{g}(\bar{\mathbf{b}}). \tag{A2.9}$$

By the implicit function theorem, there exists an interval U including 0 as an interior point and a vector-valued function of a single variable, $\bar{\mathbf{b}}(.)$: $U \to \mathbb{R}^{NF}$, such that $\mathbf{f}(\bar{\mathbf{b}}(\tilde{\gamma}), \tilde{\gamma}) = \mathbf{0}$ for all $\tilde{\gamma} \in U$ and its derivative $\bar{\mathbf{b}}'(.)$ is given by

$$\begin{aligned} \bar{\mathbf{b}}'(\tilde{\gamma}) &= -\left[\frac{\partial \mathbf{f}(\bar{\mathbf{b}}(\tilde{\gamma}), \tilde{\gamma})}{\partial \bar{\mathbf{b}}'}\right]^{-1} \frac{\partial \mathbf{f}(\bar{\mathbf{b}}(\tilde{\gamma}), \tilde{\gamma})}{\partial \gamma} \\ &= -\underbrace{\left[\mathbf{M} + \tilde{\gamma}\, \frac{\partial \mathbf{g}(\bar{\mathbf{b}}(\tilde{\gamma}))}{\partial \bar{\mathbf{b}}'}\right]^{-1}}_{(NF\times NF)} \underbrace{\mathbf{g}(\bar{\mathbf{b}}(\tilde{\gamma}))}_{(NF\times 1)} \qquad \text{(by the definition in (A2.9) of } \mathbf{f}(\bar{\mathbf{b}}, \gamma)\text{)}. \end{aligned} \tag{A2.10}$$

The solution $\bar{\mathbf{b}}(\gamma)$ can be obtained by numerically solving the differential equation (A2.10) on the interval $[0, \gamma]$ with the initial condition $\bar{\mathbf{b}}(0) = \bar{\mathbf{b}}^*$. This method, however, is computationally demanding if the dimension of the matrix to be inverted, $\mathbf{M} + \tilde{\gamma}\, \frac{\partial \mathbf{g}(\bar{\mathbf{b}}(\tilde{\gamma}))}{\partial \bar{\mathbf{b}}'}$, is large.[19] [20] An alternative is to utilize the fixed-point iteration

---

[18] Here is the expression for $\mathbf{M}^{-1}$:

$$\mathbf{M}^{-1} = \begin{bmatrix} \mathbf{I}_F & \mathbf{0} & \mathbf{0} & \dots & \mathbf{0} \\ \mathbf{\Phi}' & \mathbf{I}_F & \mathbf{0} & \dots & \mathbf{0} \\ (\mathbf{\Phi}')^2 & \mathbf{\Phi}' & \mathbf{I}_F & \dots & \mathbf{0} \\ \vdots & & \ddots & \ddots & \mathbf{0} \\ (\mathbf{\Phi}')^{N-1} & \dots & (\mathbf{\Phi}')^2 & \mathbf{\Phi}' & \mathbf{I}_F \end{bmatrix}. \tag{A2.8}$$

[19] The next section's example has $N = 80$ and $F = 1 + N$, so the size of the matrix is 6480×6480.

[20] Computation of the Jacobian $\frac{\partial \mathbf{g}(\bar{\mathbf{b}}(\tilde{\gamma}))}{\partial \bar{\mathbf{b}}'}$ is not CPU-intensive because we have an analytical expression of it. Since $\mathbf{g}(\bar{\mathbf{b}}) = \mathbf{P}\,\text{vec}(\bar{\mathbf{B}}'\mathbf{\Omega}\bar{\mathbf{B}})$ is quadratic, the Jacobian $\frac{\partial \mathbf{g}(\bar{\mathbf{b}})}{\partial \bar{\mathbf{b}}'}$ can be written as (recall: $\underset{(F\times(N-1))}{\bar{\mathbf{B}}} = [\bar{\mathbf{b}}_1, ..., \bar{\mathbf{b}}_{N-1}]$ and $\bar{\mathbf{b}}' = [\bar{\mathbf{b}}_1', ..., \bar{\mathbf{b}}_{N-1}', \bar{\mathbf{b}}_N']$)

$$\underbrace{\frac{\partial \mathbf{g}(\bar{\mathbf{b}})}{\partial \bar{\mathbf{b}}'}}_{(NF\times NF)} = \underset{(NF\times(N-1)^2)}{\mathbf{P}} \underbrace{\begin{bmatrix} \underset{((N-1)^2\times(N-1)F)}{\mathbf{A}} & \underset{((N-1)^2\times F)}{\mathbf{0}} \end{bmatrix}}_{((N-1)^2\times NF)} \tag{A2.11}$$

$$\bar{\mathbf{b}}^{(k+1)} = \mathbf{M}^{-1}[\mathbf{d} - \gamma \mathbf{g}(\bar{\mathbf{b}}^{(k)})], \quad k = 0, 1, 2, \ldots \tag{A2.13}$$

starting from $\bar{\mathbf{b}}^{(0)} = \bar{\mathbf{b}}^{*}$. This method, with no need to do numerical matrix inversion, is faster by several orders of magnitude. I have not been able to characterize a condition under which this iteration converges, though.[21] However, for numerical examples that I experimented and certainly for the example of the next section, this iteration quickly converges to the solution to the differential equation (A2.10).

---

where $\mathbf{A}$ here is

$$\underset{((N-1)^2\times(N-1)F)}{\mathbf{A}} \equiv \begin{bmatrix} \underbrace{\mathbf{I}_{N-1} \otimes \underset{(1\times F)}{\bar{\mathbf{b}}_1'} \underset{(F\times F)}{\mathbf{\Omega}}}_{((N-1)\times(N-1)F)} \\ \vdots \\ \underbrace{\mathbf{I}_{N-1} \otimes \underset{(1\times F)}{\bar{\mathbf{b}}_{N-1}'} \underset{(F\times F)}{\mathbf{\Omega}}}_{((N-1)\times(N-1)F)} \end{bmatrix} + \mathbf{I}_{N-1} \otimes \underbrace{\underset{((N-1)\times F)}{\bar{\mathbf{B}}'} \underset{(F\times F)}{\mathbf{\Omega}}}_{((N-1)\times F)}. \tag{A2.12}$$

[21] The sufficient condition identified in Poloni (2013, Theorem 4) requires that both $\mathbf{\Phi}$ and $\mathbf{\Omega}$ be nonnegative.

References

Andres, J., J. Lopez-Salido, and E. Nelson (2004): "Tobin's Imperfect Asset Substitution in Optimizing General Equilibrium, *Journal of Money, Credit and Banking*, vol. 36(4), pp. 665-90.

Bauer, Michael and Glenn Rudebusch (2014): "The Signaling Channel of Federal Reserve Bond Purchases", *International Journal of Central Banking*, September, vol. 10(3), pp. 233-289.

Bernanke, Ben (2010): "The Economic Outlook and Monetary Policy", speech at Jackson Hole, Wyoming August 2010.

Chen, Han, Vasco Curdia, and Andrea Ferrero (2012): "The Macroeconomic Effects of Large-Scale Asset Purchase Programmes", *Economic Journal*, November, pp. F289-F315.

Greenwood, Robin and Dimitri Vayanos (2014): "Bond Supply and Excess Bond Returns", *Review of Financial Studies*, January, vol. 27(3), pp. 663-713

Gurkaynak, Refet S., Brian Sack, and Jonathan H.Wright (2007): , "The U.S. Treasury yield curve: 1961 to the present", *Journal of Monetary Economics*, November, vol. 54(8), pp. 22912304.

Hamilton, James D. and Jing Cynthia Wu (2012): , "The Effectiveness of Alternative Monetary Policy Tools in a Zero Lower Bound Environment", *Journal of Money, Credit and Banking*, February, 44, pp. S3S46.

Koeda, Junko (2015): , "Bond Supply and Excess Bond Returns in Zero-Lower Bound and Normal Environments: Evidence from Japan", Working Paper 1506, Waseda University.

Poloni, Federico (2013): "Quadratic Vector Equations", *Linear Algebra and Its Applications*, 438, pp. 1627-1644.

Tobin, James (1969): "A General Equilibrium Approach to Monetary Theory", *Journal of Money, Credit and Banking*, vol.1(1), February, pp. 15-29.

Vayanos, Dimitri and Jean-Luc Vila (2009): "A Preferred-Habitat Model of the Term Structure of Interest Rates", NBER Working Paper No. 15487.

Wallace (1981): "A Modigliani-Miller Theorem for Open-Market Operations", *American Economic Review*, June, vol. 71(3), pp. 267-274.

Woodford (2012): "Methods of Policy Accommodation at the Interest-Rate Lower Bound", paper presented at the 2012 Jackson Hole conference, Federal Reserve Bank of Kansas City, September 2012.